JPE 15-4-7

http://dx.doi.org/10.6113/JPE.2015.15.4.929
ISSN(Print): 1598-2092 / ISSN(Online): 2093-4718

Single Sensor Charging System with MPPT Capability for Standalone Streetlight Applications

Siti Rahimah Osman[†,**], Nasrudin Abd. Rahim[*,***], Jeyraj Selvaraj[*], and Yusuf A. Al-Turki[***]

[†*]UM Power Energy Dedicated Advanced Centre (UMPEDAC), University of Malaya, Kuala Lumpur, Malaysia
[**]Department of Electrical Engineering, Faculty of Engineering, University of Malaya, Kuala Lumpur, Malaysia
[***]Renewable Energy Research Grouping, King Abdulaziz University, Jeddah, Saudi Arabia

Abstract

Maximum power point tracking (MPPT) and battery charging control are two important functions for a solar battery charger. The former improves utilization of the available solar energy, while the latter ensures a prolonged battery life. Nevertheless, complete implementation of both functions can be complex and costly, especially for low voltage application such as standalone street lamps. In this paper, the operation of a solar battery charger for standalone street light systems is investigated. Using only one voltage sensor, the solar charger is able to operate in both MPPT and constant voltage (CV) charging mode, hence providing high performance at a low cost. Using a lab prototype and a solar simulator, the operation of the charger system is demonstrated and its performance under varying irradiance is validated.

Key words: Battery charger, Low cost, Maximum power point tracking (MPPT), Photovoltaic (PV)

I. INTRODUCTION

Solar energy has received much attention due the fact that it is abundant, free and clean. Solar energy systems can generally be categorized into i) standalone PV systems which consist of a PV panel, battery and load; and ii) grid connected PV systems which feed additional power to the grid. Standalone PV systems are essential as they provide a power solution for remote and isolated areas which are unreachable by grid. A lot of applications involving solar energy as the sole power source have been developed to reduce the dependency on conventional energy sources. For example, street light systems consume up to 40 billion kWh of electricity annually [1]. Therefore, there is a huge potential for the use solar energy in powering these systems. By incorporating batteries and power electronics converters into solar street light systems, solar energy can be stored in the batteries during the day and used for powering the lamps during the night. Despite the attractiveness of solar street lamps, there are several major drawbacks, i.e. high installation cost and intermittency of solar irradiance. In terms of cost, solar street lights cost almost 2-4 times more than conventional systems [1]. The intermittency of solar irradiance, on the other hand, reduces the reliability of the system and has to be mitigated via oversizing the batteries and solar panels [2]. This also contributes to the high cost. Nevertheless, studies indicate that solar street lights can be a better solution in the long run in term of cost and environmental impact [1], [3], [4]. As a matter of fact, solar street lamps have been quite a successful solar product and a good selection of products is commercially available as shown in Table I.

Fig. 1 shows the typical components of a solar street light system. For a sustainable operation, the battery needs to be large enough to sustain operation over bad-sun-days, such as during rainy season. This leads to the need for increasing the size of both the solar panel and the battery. As a matter of fact, based on Table I, it has been found that the solar panels of commercial solar street lights have a rated power that is 4-7 times the lamp's power consumption, and that a high capacity battery to allow autonomous operation for up to 2-4 days.

In the past, various studies related to the technical

Manuscript received Dec. 22, 2014; accepted Apr. 5, 2015
Recommended for publication by Associate Editor Joung-Hu Park.
[†]Corresponding Author: sro.rahimah@gmail.com
Tel: +60322463246, University of Malaya
[*]UM Power Energy Dedicated Advanced Centre (UMPEDAC), University of Malaya, Malaysia
[**]Dept. of Electrical Eng., Faculty of Eng., University of Malaya, Malaysia
[***]Renewable Energy Research Grouping, King Abdulaziz University, Saudi Arabia

© 2015 KIPE

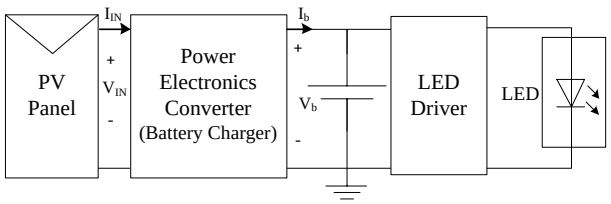

Fig. 1. Standalone solar street light system configuration.

TABLE I
VARIOUS SOLAR STREET LIGHT SYSTEM SPECIFICATIONS

	Philips	Sollatek	PCA	Hollandia
System Model	AP8	26-SOX	S80-HE X-ST 30 LED	Suntron 18W
PV panel, P_{pv} (W)	130	2x85	2x80	75
Battery Capacity, C (Ah)	150	110	2x55	100
System Voltage (V)	12	12	24	12
LED lamp (W)	29	26	30	18
Operation hours	10	10	8-10	10-12

optimization of solar street light applications have been reported [5]-[7]. Even though there are many works dedicated to the development of solar battery chargers, most of them focus on large scale power generation and high voltage applications [8]-[12]. As a result, most of the proposed systems involve the use of multiple sensors and complex algorithms which are not suitable for low voltage low cost applications. In this paper a simple solar battery charger system, suitable for standalone solar-driven low voltage applications such as solar street light systems, is studied. Using only one voltage sensor at the battery terminals, the charger is able to execute good performance MPPT and charging control. As a result, it is able to provide a low-cost and robust solution.

This paper is organized in the following manner: Section II first provides a review of solar battery charger control, with an emphasis on various battery charging control and MPPT methods. Section III presents an analysis on the single sensor battery charger control investigated in this paper. The operation of the proposed solar charger, including the transitions between the MPPT and CV modes, are explained in detail in section IV. In order to validate the suggested system, experimental results together with discussions are provided in Section V. Lastly, conclusions are stated in Section VI.

II. REVIEW ON SOLAR BATTERY CHARGER CONTROL

There are two important control tasks for solar battery chargers, i.e. battery charging control and MPPT. Charging control is important for prolonging the battery lifespan, while MPPT is crucial for maximizing energy conversion and reducing the battery charging time.

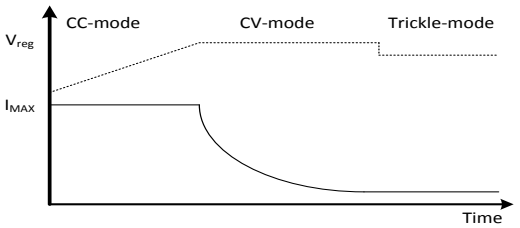

Fig. 2. V and I changes in three stage charging method.

A. Battery Charging Control

The continuous process of charging and discharging without an appropriate control can shorten the battery lifetime. Over the years, various types of battery charging systems have been developed for use with solar applications [13]–[16]. Among them, the three-stage charging method is said to be the most suitable method for photovoltaic applications [17]. The changes in voltage and current throughout the charging process are illustrated in Fig. 2. In this method, the battery is first charged in the constant current (CC) mode where the charging current is limited to around 0.2 to 0.5 of its capacity until the terminal voltage reaches the regulating charging voltage, V_{reg}. Then, the battery is charged in constant voltage (CV) mode with the terminal voltage maintained at V_{reg}. After the battery is fully charged, trickle mode is applied where the battery is charged with a voltage slightly below V_{reg} to compensate for the battery self-discharge losses. However, for lead acid batteries, self-discharge rate is low when compared to other battery technologies i.e nickel-based batteries [18]. Thus, the effect of the trickle charge mode is insignificant.

B. MPPT and Reduced Sensor MPPT

MPPT is an important issue in solar energy conversion and a comprehensive body of literature has been dedicated to its development [19]-[31]. Among the many MPPT algorithms, the Perturb and Observe (P&O) and Hill Climbing (HC) methods are the most commonly used due to their simplicity and satisfactory results [19], [20], [26]. For better performance, particularly in reducing steady state power oscillations, Incremental Conductance (InC) method is preferred [21]. In addition, more complex and computationally heavy algorithms such as Neural-Network (NN) and Fuzzy controllers have also been introduced [22], [27]. Even though these methods promise more accurate and reliable results, their complexity and long iterations make them not practical for low cost applications.

Instead of going for performance, some MPPT methods focus on reducing cost by reducing the number of sensors. Reduced sensor MPPT has been proposed in many previous studies in an effort to provide low cost and simpler MPP tracking systems. [24], [28]-[31] proposed reduced MPPT algorithms at the PV panel side. Either PV voltage or PV current parameter is used to estimate the value of the power

generated by PV panel. On the other hand, [23] introduced a MPP tracking algorithm via output parameters i.e load power, load voltage and load current. By comparing these three parameters, the load current parameter tracking has the highest MPPT efficiency. Shmilovitz (2005) has initiated a lot of research on load current MPPT. In [25], the conventional load current MPP was improved by adding an adaptive step size and adaptive perturbation frequency to further improve the efficiency of the algorithm. In another work, the load current MPPT algorithm was introduced in solar battery charging system which further reduced the whole system cost and complexity while providing similar system performance when compared to conventional systems [32]. However, the load voltage MPP tracking algorithm has not been further explored. This paper explored the use of the load voltage MPP tracking algorithm in solar battery chargers.

III. Single Sensor Solar Battery Charger

For standalone solar street light systems, such as those listed in Table 1, a large battery is matched with a relatively small PV panel. Assuming that an ideal power converter is used, a maximum charging current, I_{MAX} occurs only during MPP and generally should not exceed 0.2 of the battery's capacity. This constrain can be expressed in terms of the panel power, P_{in} and battery capacity, C as:

$$I_{MAX} = \frac{P_{in}}{V_{batt}} < 0.2C \tag{1}$$

Based on Table 1, it is found that I_{MAX} varies from 0.06C to 0.12C, which satisfies constrain (1). This shows that even at its best performance, PV panel is unable to deliver a maximum charging current to the battery. Since the system never exceed the maximum charging current, the need for current control in the charging algorithm can be eliminated. Thus, the conventional three-stage charging method can be modified by replacing the CC-mode with MPPT mode and eliminating the third charging stage, i.e. the trickle charging stage. This gives rise to the MPPT-CV charging method, which eliminates the current sensor at the battery side. During MPPT mode, the system extracts the maximum power from the solar power and maximizes the charging current to speed up the charging process. When the battery voltage reaches V_{reg}, the system will then transit into CV mode to avoid overcharging.

Since only the battery voltage sensor remains, a MPPT technique utilizing the load voltage parameter is applied. Here, an output voltage sensing MPPT technique is adopted for the solar charger. As a result, both the MPPT and battery charging control can be achieved by utilizing only one voltage sensor at the battery terminals. The concept of a single output voltage sensing MPPT is explained here. First assume that the battery charger is an ideal power converter, i.e.:

$$P_{in} = P_{out} = V_b I_b \tag{2}$$

From (2) the changes in the input power and output power with respect to the duty cycle D can be represented by:

$$\frac{dP_{in}}{dD} = \frac{d(I_b V_b)}{dD} \tag{3}$$

The dynamic battery model [33] is used to model the lead-acid battery here. The model consists of a voltage source, E in series with an internal resistance, R_{int}. Note that R_{int} represents the resistance due to the ESR and other stray resistances exist between the charger and the battery. Thus, the battery voltage, V_b and current, I_b can be expressed as:

$$V_b = E + R_{\text{int}} I_b \tag{4}$$

where both E and R_{int} are functions of the state of charge (SOC), which depends on the charging current:

$$SOC = SOC_{initial} + \frac{\int I_b dt}{C_{norm}} \tag{5}$$

In the short period of time during MPPT, the change in the SOC is negligible. Therefore, E and R_{int} can be considered as constants. Thus, taking the derivative of I_b with respect to the duty cycle D will yield:

$$\frac{dI_b}{dD} = \frac{1}{R_{\text{int}}}\left(\frac{dV_b}{dD}\right) \tag{6}$$

Equation (2) can be expanded into:

$$\frac{dP_{in}}{dD} = \left(\frac{V_b dI_b}{dD} + \frac{I_b dV_b}{dD}\right) \tag{7}$$

Substituting (6) into (7) gives the following equation:

$$\frac{dP_{in}}{dD} = \left(I_b + \frac{V_b}{R_{\text{int}}}\right)\frac{dV_b}{dD} \tag{8}$$

Since all of the parameters in the brackets are always positive, the change in P_{in} with respect to D is proportional to the change in V_b with respect to D. Hence, the MPP can be tracked with a concept similar to the HC method, with the aim of maximizing the battery terminal voltage instead of the PV power.

IV. System Analysis

A. Buck Converter as a Solar Battery Charger

In a solar street light system (Fig. 1), a DC/DC converter serves as the battery charger and performs the charging control and MPPT. Among the many DC/DC converter topologies available, buck converters and boost converters are considered to be the simplest converters in their class and they exhibit high power conversion efficiency [34]. Boost converters are well suited in PV systems with series connected batteries which have a voltage that is higher than V_{PV} [35]. In low voltage

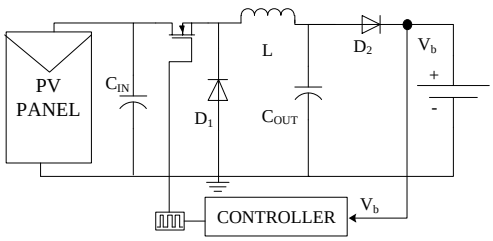

Fig. 3. Buck converter as solar battery charger.

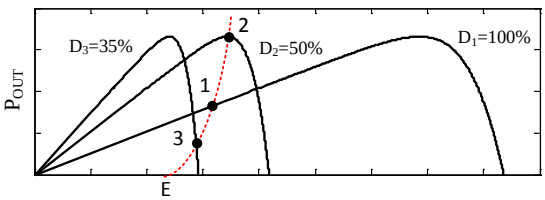

Fig. 4. Changes of duty cycle effect on PV panel operating point.

applications such as solar street lights, buck converter topology is preferred. Here, a solar battery charging system using a buck converter is considered.

It is worth mentioning that the major drawback of the buck converter is that once V_{in} falls below the battery voltage, the solar panel will no longer be able to charge the battery. Nevertheless, this can be avoided by having a higher rating PV panel, which is common for solar street lamps as observable from Table I. A schematic for a solar battery charging system using a buck converter is illustrated in Fig. 3. A reverse block diode (D_2) is added to ensure unidirectional current flow to the battery. Since D_2 causes a constant voltage drop, it is placed before the voltage sensor to avoid any errors in battery voltage measurement.

The operation of the battery load connected to a solar panel via a buck converter can be illustrated using a power-voltage (*P-V*) curve, as seen in Fig. 4. It should be mentioned here that instead of showing the input *P-V* variation (from the solar panel's perspective) as with most studies, the analysis here is done from the battery's perspective, i.e. the output *P-V* variation is shown. This is because the output parameters, particularly the battery voltage, are more important than the input parameters in this case. Analysis from the output end will facilitate better understanding of the battery's condition, particularly for transitions between MPPT and CV modes.

From (2) and (4), the battery's load characteristic can be described by:

$$P_{out} = V_b \frac{(V_b - E)}{R_{\text{int}}} \tag{9}$$

This is practically a quadratic line on the *P-V* plot with the *x*-axis intercept being *E*, as indicated by the dotted line in Fig. 4. Due to the presence of a buck converter, the *P-V* curve of the solar panel as seen by the battery is a function of *D*. Under constant irradiance, increasing *D* shifts the curve to the right, while reducing *D* moves it to the left. Since the converter is assumed to be ideal, the maximum power remains the same regardless of *D*.

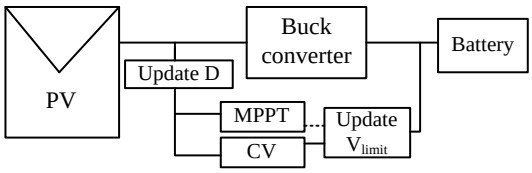

Fig. 5. Control block for the developed solar battery charger.

The operating point of a solar panel depends on the intersection between the load line and *P-V* curve of that solar panel. At point 1 (*D*=100%), the battery is considered to be directly coupled with the PV panel and the operating point lies on the left side of the MPP. The operating point can be shifted to the MPP (point 2), by decreasing *D* to 50%, to harvest the maximum power from the panel. If *D* is further decreased to D_3, the operating point shifts to the right of the MPP (point 3) and the battery harvests less power from the PV panel.

It is worth noting that when not operating at the MPP, there are two possible cases for the operating point. Either it is on the left of the MPP (operating point 1 in Fig. 4), or it is on the right of the MPP (operating point 3 in Fig. 4). As a matter of fact, there can be two different values of *D* which give the same power and same battery voltage, with the system operating on different sides of the MPP. For the hill climbing method with a fixed step, operation on the left of the MPP gives lower power oscillation than operation on the right of the MPP. This is due to the lower steepness of the *P-V* slope on the left than the right of the MPP. Hence, the system should try to operate on the left of the MPP whenever possible.

B. Operation in MPPT Mode

Fig. 5 shows the control block for the developed solar battery charger. The system continuously updates the battery voltage and switches between MPPT and CV modes. The MPPT-CV charging algorithm flow chart is illustrated in Fig.6. $V_b(k)$ and $D(k)$ are the charging voltage and buck converter duty cycle at the *k*-th iteration, respectively. The system step size, ΔD is fixed at 0.02 and the variable ΔV is the subtraction of $V_b(k)$ from V_{reg}. Initially, ΔV is determined to decide whether the system should operate in MPPT mode or CV mode. As long as ΔV is negative, i.e. the voltage limit is not exceeded, the system should operate in MPPT mode. Using the hill climbing concept, the battery voltage is compared with its previous value to determine the change in the duty cycle so that the MPP can be tracked. The MPPT algorithm is illustrated by the blue dotted box in Fig. 6.

C. Operation in CV Mode

Based on the MPPT-CV algorithm, the system transits into CV mode whenever ΔV is positive, i.e. when battery voltage exceeds V_{reg}. This usually occurs when the level of irradiance is high. Unlike fixed load, the battery load line

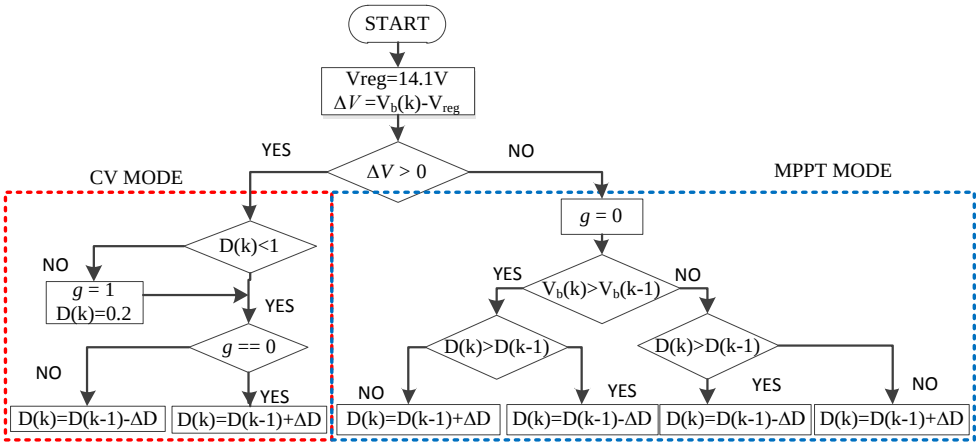

Fig. 6. Complete battery charging control algorithm.

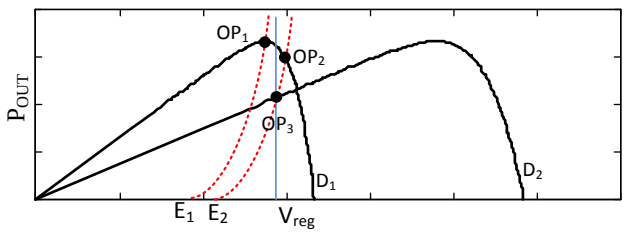

Fig. 7. Changes of battery load line effect on PV operating point.

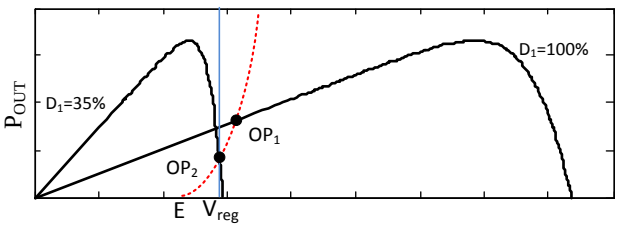

Fig. 8. Changes of battery load line effect in CV mode.

changes with the battery's SOC, due to its effect on E and R_{int}. With a constant D and a constant irradiance, the operating point may still move due to changes in E. This situation can be explained using Fig. 7. Initially, the battery has an internal voltage of E_1, and the system is able to operate at the MPP (at OP_1) without exceeding V_{reg}. However, as the charging process continues, the battery load line shifts to the right (the battery load line crossing at E_2) as seen from Fig. 7. At this point (OP_2), battery voltage is above V_{reg}. To prevent the battery from overcharging, duty cycle is increased to D_2 to bring the operating point to OP_3, and maintain battery voltage at V_{reg}. It is possible to bring the voltage down by reducing D and operating on the right side of the MPP. However, as mentioned earlier, operating on the left of the MPP gives lower oscillations and is preferred. Under certain circumstances, increasing D to its maximum, (D=100%) is still insufficient to bring the charging voltage down to V_{reg}. This is illustrated in Fig. 8, where even with D=100% the battery voltage is still higher than V_{reg} (at OP_1). Since D can no longer be increased, it will have to be drastically reduced to bring the operating point to the right side of the MPP to avoid overcharging. It can be observed that if D is gradually decreased from 100% to 35%, the battery voltage will increases before decreasing. This is very undesirable as it results in prolonged overvoltage operation. To avoid this, it is proposed that whenever the maximum duty cycle is detected in CV mode, D should be drastically reduced. In this way, the operating point "jumps" to the right of the MPP, and reaches V_{reg} faster. The algorithm for CV-mode of operation is given by the red dotted box in Fig. 6. The variable g is used to determine the location of the operating point. g=0 indicates operation on the left of the MPP, while g=1 designates operation on right of the MPP. The CV-mode operation starts by checking D. For D below maximum (D<100%), variable g is set to 0 and the operating point oscillates on the left side of the MPP. If D reaches 100%, g is set to 1 to mark the jump of the operating point and D will be drastically reduced to operate at the right side of the MPP.

D. Other Considerations

One important implementation challenge of this method is the accuracy of the voltage sensing circuit. Since the changes in battery voltage are relatively small, an additional circuit is required to increase the sensitivity of the system. The battery voltage under normal discharging and charging processes varies from 10 V to 15V while a normal sensor is able to sense voltage with the lower limit set to zero. A differential amplifier circuit is used for amplification propose which increase the sensitivity of the system. Having a narrow perturbation band, the system is susceptible to noise and it can mistakenly treat noise as a perturbation signal. Due to that, data from the voltage sensor are averaged and sampled before the voltage signal is use as $V_b(k)$ in the battery charging algorithm.

V. Results and Discussion

The proposed single sensor solar battery charger system is validated experimentally. The experimental setup consists of a

TABLE II
SUMMARY OF ALL SYSTEM PARAMETERS

PV Panel	
Power rating	175Watt
Voltage open circuit, V_{oc}	44.2V
Short circuit current, I_{sc}	5.2A
V_{mpp} at 1000W/m^2	35.2V
I_{mpp} at 1000W/m^2	4.95A
Controller	
Sampling rate	100ms
Switching frequency	100kHz
Battery specification	
Technology	VRLA
Voltage	12V
Capacity	80Ah
Regulation Voltage, V_{reg}	14.1 V

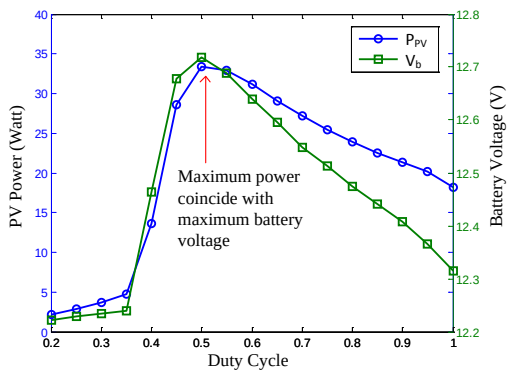

Fig. 9. PV power generated and battery voltage versus sweep of buck converter duty cycle.

solar emulator (Chroma Programmable DC supply 62150H-1000S), a buck converter and a lead acid battery, as shown in Fig. 3. A low cost PIC18F4553 microcontroller is used in this system. The parameters of the experimental setup are summarized in Table II. The experimental results are captured using a Tektronix TDS 2014C oscilloscope.

A. Verification of Voltage and Power Relation

In previous research, the battery voltage is usually treated as a constant, [32]. In Section IV, an analysis on the changes in the battery voltage and PV power has shown a proportional relationship between the two variables, as indicated in (8). This conclusion is verified experimentally by sweeping the duty cycle of the buck converter from 0 to 1 while keeping the irradiance at 200W/m^2. The PV power generated and the battery charging voltage are plotted as in Fig. 8. It is clear that the PV power changes proportionally with the battery voltage, such that the maximum power coincides with the maximum battery voltage. Hence, MPPT can be tracked using battery voltage as the perturbation parameter instead of the PV power.

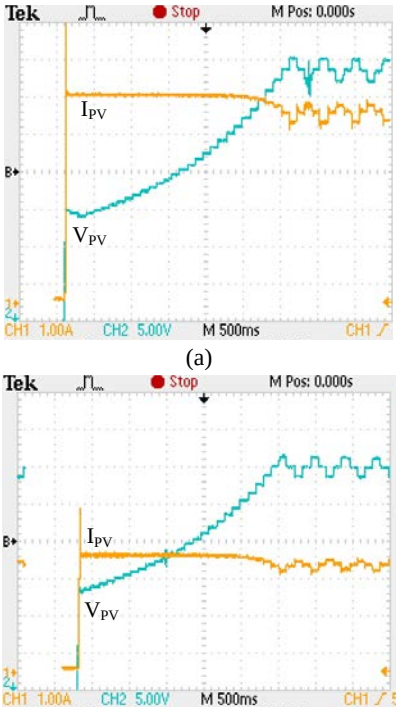

Fig. 10. PV voltage and current during MPPT at a) 1000 W/m^2 b) 500W/m^2.

B. MPPT Performance under Constant and Sudden Change of Irradiation

Fig. 10(a) and 10(b) show the voltage and current responses of the PV panel during the MPPT mode at irradiance of 1000W/m2 and 500W/m2, respectively. It can be seen that the proposed algorithm is able to reach MPP using only the battery voltage as the perturbation parameter. Steady state oscillations for both and current and voltage are also evident in both Fig. 10(a) and Fig. 10(b). These oscillations are characteristic of the constant step HC method.

In Fig. 11(a) and 11(b) the system is tested for sudden change of irradiance. It is observed that the system is able to track the new MPP for both sudden drops and sudden increases of irradiance within a short period of time.

C. Transition between MPPT and CV Modes

As the charging process continues, the charging voltage increases. In order to prevent premature failure of the battery, it is vital to keep the charging voltage below V_{reg}, which is 14.1 V in this case. In the proposed system, the solar charger operates in MPPT mode until the battery voltage reaches 14.1V, after which the system will operate in CV mode to keep the battery voltage at its limit. Fig. 12 shows the transition from CV mode to MPPT mode. Initially, the battery voltage is at 14.1V, where the charger operates in the CV mode. When there is a sudden drop of irradiance, there is also a large and abrupt drop in the battery current. As a result, the battery voltage reduces below 14.1V, and the charger

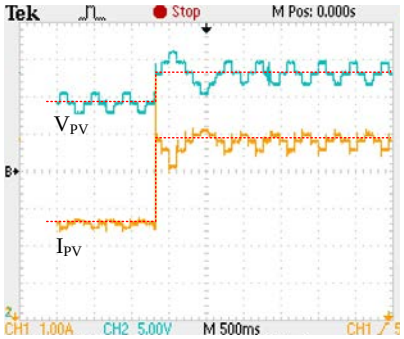

(a)

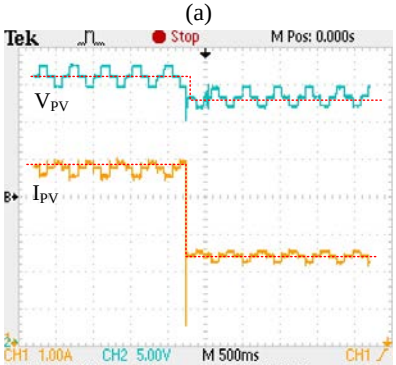

(b)

Fig. 11. PV voltage and current response during sudden change of irradiance from a) 500W/m^2 to 1000W/m^2 b) 1000W/m^2 to 500W/m^2.

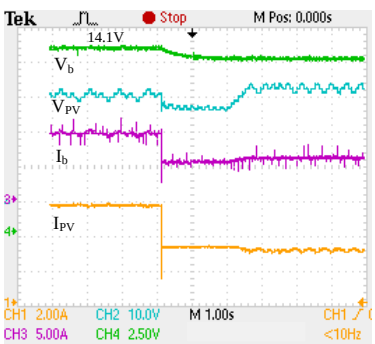

Fig. 12. Transition from CV to MPPT mode.

transits into MPPT mode. However, due to the slow chemical reaction within the lead-acid battery, the battery voltage drop is gradual under a sudden irradiance drop, as evident in Fig 12. During this period of time, the voltage drop due to the battery's chemistry is larger than the voltage change due to duty cycle perturbations at the Buck converter. As a result, there is a net reduction in the battery voltage seen by the MPPT controller. Based on the MPPT algorithm, the controller tries to increase the battery voltage by changing the direction of the perturbation. However, the new perturbation is still masked by the gradual voltage drop, and the controller still sees a net reduction in the battery voltage. This causes the MPPT algorithm to keep inverting the direction of perturbation. Eventually, when the voltage transient due to battery's chemistry finally dies out, the Buck converter is once again able to control the battery voltage. The controller

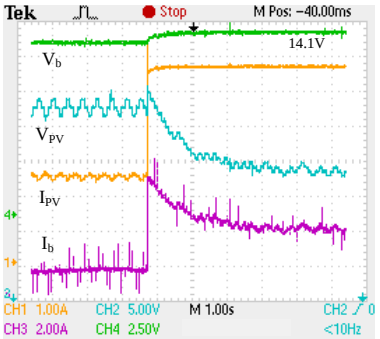

Fig. 13. Transition from MPPT to CV mode.

then drives the battery voltage up to achieve MPPT.

Transition from MPPT to CV occurs when there is a sudden increase in irradiance and the battery is partially full. When a sudden increase of irradiance occurs, the system tries to track the new MPP. However, with the gradual increment caused by the chemical reaction within the battery, the system misinterprets the voltage increment as a MPPT perturbation step. This explains the continuous drop of V_{PV} even when the battery voltage is increasing as shown in Fig.13. This indicates that duty cycle changes have no effect on the battery voltage before it is stabilized. When the battery voltage stabilizes at around 14.1V, the system switches to CV mode and maintain the charging voltage at 14.1V. Nevertheless, the battery charging voltage is still within its set limits for both mode transitions (MPPT to CV mode and vice versa). A deficiency in the charging process during this short period of time has a marginal effect on the system performance. Thus, the delay has no negative impact to the charging process.

D. Operation under Real Weather Conditions

In order to confirm the robustness of the system, a whole day of testing under real weather condition is performed. In this test, real weather data is fed into a solar simulator to emulate the solar panel performance under real weather conditions. The weather data from a cloudy day in Kuala Lumpur, Malaysia is used to test the system performance under relatively poor weather condition. For this test, the battery is first discharged until its terminal voltage dropped to 11.7V. This is to emulate a partially discharged battery condition similar to the conditions found in street a lamp system at the beginning of a day.

The charging started at around 9am, when the solar irradiance is sufficient high to facilitate charging. Initially, the system operates in MPPT mode, which can be observed from region 1 of Fig. 14(a) where the PV current, I_{PV} follows closely the pattern of the MPP current, I_{mpp}. Good tracking can be observed even under a varying irradiance as the MPPT efficiency remains high throughout MPPT mode, confirming the robustness of the MPPT algorithm. As the battery voltage reaches V_{reg} at around 12:45pm, the system transits into CV mode (as indicated by region 2 in Fig. 14(b)) such that the

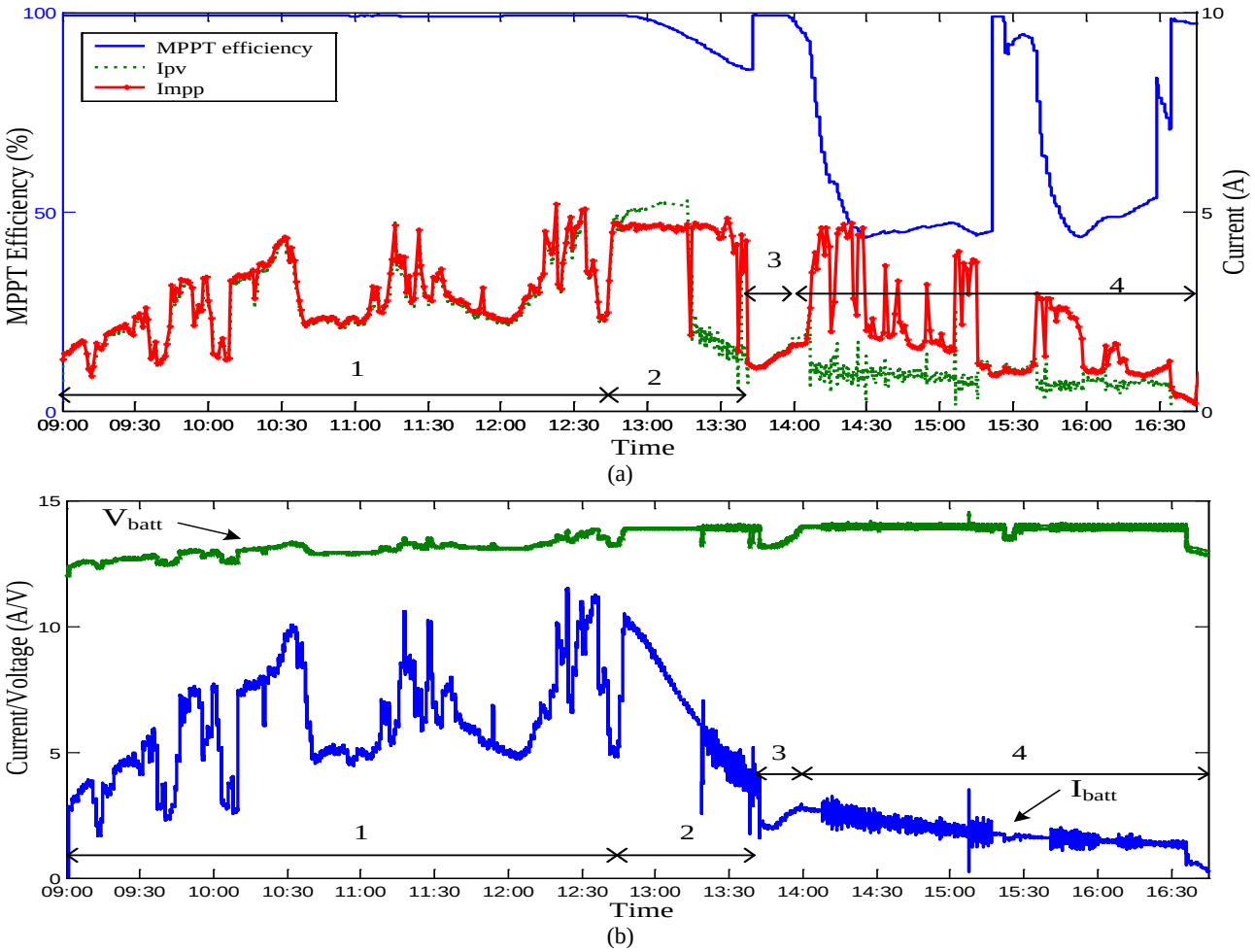

Fig. 14. Experimental results for one day testing shows the waveform. (a) MPPT efficiency, I_{PV} and I_{MPP} of the PV panel. (b) Charging voltage and charging current of the battery.

charging voltage is regulated at around 14.1V to avoid overcharging. At this point, the charger is only drawing a fraction of the solar panel's maximum power, which is reflected by the falling MPPT efficiency in Fig. 14(a).

During this stage of charging, it can be observed that the battery charging current quickly drops from approximate 10A at 12:45 to about 4A at 13:45. This indicates that the battery is reaching its full charge capacity. It is observed that while operating in region 2, i.e. CV-mode, larger oscillations in both battery voltage and current appears in the latter half of region 2 (around 13:15 to 13:45). This is due to the change of the operating point from the left side to the right side of the MPP.

Note that the left and right side of the MPP have different amounts of steepness with right side of the MPP having a steeper gradient. Since the system is operating at a constant step size the different steepness will be reflected as larger oscillations for both current and voltage of the battery when the PV panel is operating at the right side of the MPP. However, the oscillation in voltage is not significant and charging voltage is still retained within its set limit.

When irradiance suddenly falls at around 13:45pm, the PV power is reduced as well. Hence, the controller switches back to MPPT mode to maximize the power drawn from the PV panel (region 3). Subsequently, the system continues to alternate between CV and MPPT modes for the remaining time (region 4), until the sun goes out at around 5pm. A similar oscillation rate can be observed in region 4 which is also resulted from the movement of the operating point. As the charging process continues, a noticeable spike is observed in the voltage and current reading in the middle of region 4 due to the sudden change of irradiance. However, the spike occurred for a very short time and is around 14.5V, which is slightly above the maximum allowable charging voltage (14.4V). Thus, this does not affect the battery performance. At the end of the charging process, I_{batt} drops to around 1A towards the end of operation time indicating that the battery is almost fully charged despite the poor weather conditions.

Overall, the system is found to perform well under actual weather conditions, where it switches between MPPT and CV modes to maximize charging of the battery while maintaining the battery voltage within the allowable limit. During MPPT

operation, the MPPT efficiency is found to be around 97%. This confirms the effectiveness of the single sensor MPPT method proposed in this paper. It is worth noting that the MPPT efficiency drops during CV mode the system is trying to maintain a constant charging voltage instead of operating at the MPP.

VI. CONCLUSIONS

In this paper, the operation of a single sensor battery charger in street light applications is analyzed and developed. Using only one voltage sensor on the battery terminals, the solar charging system is able to perform both battery charging control and MPPT control, hence providing a simple and low cost solution for solar battery chargers. Depending on the battery voltage and solar irradiation, the proposed control switches between MPPT and CV modes, maximizing the power extracted from solar panel without compromising the battery's health. Experimental results confirm the performances of the overall battery charger control.

ACKNOWLEDGMENT

This project is funded by PV105-2012A research grant from IPPP, University of Malaya and HIR grant H-16001-00-D000032 (Campus network smart grid system for energy security).

REFERENCES

[1] G. Liu, "Sustainable feasibility of solar photovoltaic powered street lighting systems," *Int. J. Electr. Power Energy Syst.*, Vol. 56, pp. 168-174, Mar. 2014.

[2] R. Panguloori, P. Mishra, and S. Kumar, "Power distribution architectures to improve system efficiency of centralized medium scale PV street lighting system," *Sol. Energy*, Vol. 97, pp. 405-413, Nov. 2013.

[3] N. R Velaga and A. Kumar, "Techno-economic evaluation of the feasibility of a smart street light system: a case study of rural India," *Procedia - Soc. Behav. Sci.*, Vol. 62, pp. 1220-1224, Oct. 2012.

[4] M. S. Wu, H. H. Huang, B. J. Huang, C. W. Tang, and C. W. Cheng, "Economic feasibility of solar-powered led roadway lighting," *Renew. Energy*, Vol. 34, No. 8, pp. 1934-1938, Aug. 2009.

[5] O. S. Sastry, V. Kamala Devi, P. C. Pant, G. Prasad, R. Kumar, and B. Bandyopadhyay, "Development of white LED based PV lighting systems," *Sol. Energy Mater. Sol. Cells*, Vol. 94, No. 9, pp. 1430-1433, Sep. 2010.

[6] B.-J. Huang, C.-W. Chen, P.-C. Hsu, W.-M. Tseng, and M.-S. Wu, "Direct battery-driven solar LED lighting using constant-power control," *Sol. Energy*, Vol. 86, No. 11, pp. 3250-3259, Nov. 2012.

[7] B. J. Huang, M. S. Wu, P. C. Hsu, J. W. Chen, and K. Y. Chen, "Development of high-performance solar LED lighting system," *Energy Convers. Manag.*, Vol. 51, No. 8, pp. 1669-1675, Aug. 2010.

[8] N. a. Kelly and T. L. Gibson, "Increasing the solar photovoltaic energy capture on sunny and cloudy days," *Sol. Energy*, Vol. 85, No. 1, pp. 111-125, Jan. 2011.

[9] H.-I. Hsieh and G.-C. Hsieh, "A study of high-frequency photovoltaic pulse charger for lead-acid battery guided by PI-INC MPPT," in *2012 International Conference on Renewable Energy Research and Applications (ICRERA)*, 2012, Vol. 1, pp. 1-6.

[10] M. Bortolini, M. Gamberi, and A. Graziani, "Technical and economic design of photovoltaic and battery energy storage system," *Energy Convers. Manag.*, Vol. 86, pp. 81-92, Oct. 2014.

[11] M. Z. Daud, A. Mohamed, and M. A. Hannan, "An improved control method of battery energy storage system for hourly dispatch of photovoltaic power sources," *Energy Convers. Manag.*, Vol. 73, pp. 256-270, Sep. 2013.

[12] S. Park, J. Shin, J. Park, and H. Jeon, "Dynamic analysis and controller design for standalone operation of photovoltaic power conditioners with energy storage," *J. Electr. Eng. Technol.*, Vol. 9, pp. 742-750, 2014.

[13] E. Koutroulis and K. Kalaitzakis, "Novel battery charging regulation system for photovoltaic applications," in *Electric Power Applications, IEE Proceedings*, pp. 191-197, 2004.

[14] M. Bhatt, W. G. Hurley, S. Member, and W. H. Wölfle, "A new approach to intermittent charging of valve-regulated lead - acid batteries in standby applications," *IEEE Trans. Ind. Electron.*, Vol. 52, No. 5, pp. 1337-1342, Oct. 2005.

[15] H. Hsieh, C. Tsai, and G. Hsieh, "Photovoltaic burp charge system on energy-saving configuration by smart charge management," *IEEE Trans. Power Electron.*, Vol. 29, No. 4, pp. 1777-1790, Apr. 2014.

[16] D. Fendri and M. Chaabene, "Dynamic model to follow the state of charge of a lead-acid battery connected to photovoltaic panel," *Energy Convers. Manag.*, Vol. 64, pp. 587-593, Dec. 2012.

[17] S. Armstrong, M. E. Glavin, and W. G. Hurley, "Comparison of battery charging algorithms for stand alone photovoltaic systems," in *2008 IEEE Power Electronics Specialists Conference*, 2008, pp. 1469-1475.

[18] B. W. Williams, *Power electronics: devices, drivers, applications, and passive components*. Glasgow, 2006, p. 1020.

[19] N. Femia, G. Petrone, G. Spagnuolo, and M. Vitelli, "Optimization of perturb and observe maximum power point tracking method," *IEEE Trans. Power Electron.*, Vol. 20, No. 4, pp. 963-973, Jul. 2005.

[20] B. Subudhi and R. Pradhan, "A comparative study on maximum power point tracking techniques for photovoltaic power systems," *IEEE Trans. Sustain. Energy*, Vol. 4, No. 1, pp. 89-98, Jan. 2013.

[21] M. A. Elgendy, B. Zahawi, and D. J. Atkinson, "Assessment of the incremental conductance maximum power point tracking algorithm," *IEEE Trans. Sustain. Energy*, Vol. 4, No. 1, pp. 108-117, Jan. 2013.

[22] Z. Salam, J. Ahmed, and B. S. Merugu, "The application of soft computing methods for MPPT of PV system: A technological and status review," *Appl. Energy*, Vol. 107, pp. 135-148, Jul. 2013.

[23] D. Shmilovitz, "On the control of photovoltaic maximum power point tracker via output parameters," in *Electric Power Applications, IEE Proceedings*, 2005, pp. 239 - 248.

[24] A. Pandey, N. Dasgupta, and A. K. Mukerjee, "A simple single-sensor MPPT solution," *IEEE Trans. Power Electron.*, Vol. 22, No. 2, pp. 698-700, Mar. 2007.

[25] Y. Jiang, S. Member, J. A. A. Qahouq, S. Member, and T. A. Haskew, "Adaptive step size with adaptive-perturbation-frequencydigital MPPT controller for a single-sensor

photovoltaic solar system," *IEEE Trans. Power Electron.*, Vol. 28, No. 7, pp. 3195-3205, Jul. 2013.
[26] D. P. Hohm and M. E. Ropp, "Comparative study of maximum power point tracking algorithms," *Prog. Photovoltaics Res. Appl.*, Vol. 11, No. 1, pp. 47-62, Jan. 2003.
[27] O. Guenounou, B. Dahhou, and F. Chabour, "Adaptive fuzzy controller based MPPT for photovoltaic systems," *Energy Convers. Manag.*, Vol. 78, pp. 843-850, Feb. 2014.
[28] V. Salas, E. Olías, a. Lázaro, and a. Barrado, "New algorithm using only one variable measurement applied to a maximum power point tracker," *Sol. Energy Mater. Sol. Cells*, Vol. 87, No. 1-4, pp. 675-684, May 2005.
[29] N. Dasgupta, a Pandey, and a Mukerjee, "Voltage-sensing-based photovoltaic MPPT with improved tracking and drift avoidance capabilities," *Sol. Energy Mater. Sol. Cells*, Vol. 92, No. 12, pp. 1552-1558, Dec. 2008.
[30] M. Momayyezan and H. Iman-eini, "Developed MPPT algorithm for photovoltaic systems without a voltage sensor," *Journal of Power Electronics*, Vol. 13, No. 6, pp. 1042-1050, Nov. 2013.
[31] D. Ryu, B. Choi, S. Lee, Y. Kim, and C. Won, "Flyback inverter using voltage sensorless MPPT for photovoltaic AC modules," *Journal of Power Electronics*, Vol. 14, No. 6, pp. 1293-1302, Nov. 2014.
[32] T.-T. Nguyen, H. W. Kim, G. H. Lee, and W. Choi, "Design and implementation of the low cost and fast solar charger with the rooftop PV array of the vehicle," *Sol. Energy*, Vol. 96, pp. 83-95, Oct. 2013.
[33] H. L. Chan, "A new battery model for use with battery energy storage Systems and electric vehicles power systems," *Power Eng. Soc. Winter Meet. 2000. IEEE*, Vol. 1, pp. 470 - 475, 2000.
[34] M. H. Taghvaee, M. a. M. Radzi, S. M. Moosavain, H. Hizam, and M. Hamiruce Marhaban, "A current and future study on non-isolated DC-DC converters for photovoltaic applications," *Renew. Sustain. Energy Rev.*, Vol. 17, pp. 216-227, Jan. 2013.
[35] Y. Du and D. D.-C. Lu, "Battery-integrated boost converter utilizing distributed MPPT configuration for photovoltaic systems," *Sol. Energy*, Vol. 85, No. 9, pp. 1992-2002, Sep. 2011.

Siti Rahimah Osman received her B.S. degree in Engineering from Universiti Teknologi Malaysia (UTM), Kuala Lumpur, Malaysia, and is presently working towards her M.S. degree at UM Power Energy Dedicated Advanced Centre (UMPEDAC), University of Malaya, Kuala Lumpur, Malaysia. Her current research interests include PV systems, reduced sensor MPPT, energy storage and battery management systems.

Nasrudin Abd. Rahim (M'89-SM'08) received his B.S. (Hons.) and M.S. degrees from the University of Strathclyde, Glasgow, Scotland, UK, and his Ph.D. degree from Heriot-Watt University, Edinburgh, Scotland, UK, in 1995. He is presently working as a Professor at the University of Malaya, Kuala Lumpur, Malaysia, where he is also the Director of the UM Power Energy Dedicated Advanced Centre (UMPEDAC). He is also an Adjunct Professor at King Abdulaziz University, Jeddah, Saudi Arabia. His current research interests include power electronics, Solar PV and wind technologies, real-time control systems, and electrical drives. Professor N.A Rahim is a Senior Member of the IEEE and a Fellow of both the Institution of Engineering and Technology, UK, and the Academy of Sciences Malaysia. He is also a Chartered Engineer (UK)

Jeyraj Selvaraj received his B.S. (Hons.) degree in Engineering from the Multimedia University, Cyberjaya, Malaysia, in 2002, his M.S. degree in Power Electronics and Drives jointly from the University of Birmingham, Birmingham, England, UK, and the University of Nottingham, Nottingham, England, UK, in 2004, and his Ph.D. degree from the University of Malaya, Kuala Lumpur, Malaysia, in 2009. He is presently with the Power Energy Dedicated Advanced Centre (UMPEDAC), University of Malaya. His current research interests include single-phase and three-phase multilevel inverters, digital current-control techniques, photovoltaic inverters, and dc-dc converters.

Yusuf A. Al-Turki received his B.S. degree in Electrical Engineering from the Department of Engineering, King AbdulAziz University, Jeddah, Saudi Arabia, and his Ph.D. in Power Engineering from the University of Manchester, Manchester, England, UK. He is presently working as a Professor in the Department of Electrical and Computer Engineering, Faculty of Engineering, King Abdulaziz University.